Influence of time- and depth-dependent eddy viscosity on the formation of tidal sandwaves

P. C. Roos[(1)], H. M. Schuttelaars[(2)]

1. Water Engineering and Management, University of Twente, Enschede, Netherlands – p.c.roos@utwente.nl
2. Delft Institute of Applied Mathematics, Delft University of Technology, Delft, Netherlands – h.m.schuttelaars@tudelft.nl

Abstract

Existing model studies on sandwave dynamics point to the importance of turbulence, and particularly its temporal and spatial structure. We present an idealized model of sandwave formation, in which turbulence is accounted for by adopting a time- and depth-dependent eddy viscosity. Following linear stability analysis, the basic and perturbed flow solutions are obtained using a spectral method involving eigenfunctions that simplify the vertical stress term. First model results show favourable convergence properties of the basic state, expressing the generation of higher harmonics due to the time-dependent eddy viscosity. The perturbed state, which requires further investigation in detail, reveals large flow gradients close to the bed.

1. INTRODUCTION

1.1. Tidal sandwaves

Tidal sandwaves are dynamic bed forms observed in tide-dominated shallow seas, characterized by wavelengths of hundreds of meters, heights of several meters and migration rates up to tens of meters per year. Sandwaves may pose a hazard to navigation and the safety of pipelines and wind farms. Understanding sandwave dynamics thus helps improving/optimizing the design and maintenance of pipelines and wind farms, the dredging operations in approach channels and the survey strategies for nautical charting.

1.2. Sandwave modelling

Tidal sandwaves have been explained as an inherent instability of a flat seabed subject to tidal motion (Hulscher 1996). Wave-like bottom undulations perturb the water motion such that vertical residual circulation cells are formed with a near-bed flow directed from trough to crest. If sufficiently strong to overcome gravity, this flow transports sediment from trough to crest, thus causing the undulation to grow. This formation process was described by a linear stability analysis, which produces growth rates as a function of the topographic wave number k and orientation with respect to the tidal current. Instability is expressed by the occurrence of positive growth rates, the maximum of the growth curve defines the so-called fastest growing mode. Hulscher (1996) considered symmetric tidal forcing, a schematized turbulence model (constant and uniform vertical eddy viscosity with partial slip at the bed) and bed load transport. Later on, this model was extended to explain sandwave migration due to residual currents and overtides in the forcing (Németh et al. 2002, Besio et al. 2004), role of higher harmonics in the perturbed flow (Gerkema 2000, Besio et al. 2003a) and the representation of turbulence and suspended load transport (Blondeaux & Vittori 2005ab). Although the characteristics of the fastest growing mode generally agree with observations from e.g. the North Sea, these linear models suffer from two shortcomings: (*i*) their validity is restricted to small amplitudes and (*ii*) they fail to

suppress the growth of 'ultra-long' sandwaves (near $k = 0$).

The first shortcoming, actually a restriction of linear stability analyses in general, has inspired the development of nonlinear models. (e.g., Németh et al. 2007, Sterlini et al. 2009). These models describe sandwave evolution towards equilibrium, but the modelled equilibrium heights exceed those observed in the field. Furthermore, simulations of patterns with multiple sandwaves (on a spatially periodic domain) ultimately develop into a single feature with a wavelength equal to the length of the computational domain. This is physically unrealistic and probably related to the second shortcoming, i.e. the failure of suppressing ultra-long sandwaves.

1.3. Turbulence representation

Resolving this problem requires a closer investigation of the representation of turbulence and sediment transport. Komarova & Hulscher (2000) showed that adopting a time-dependent eddy viscosity of a particular form helps to suppress the growth of very long sandwaves. They considered bed load transport and continued to use the schematized turbulence model with a uniform eddy viscosity and partial slip at the bed. Although computationally appealing (basic flow analytically available), it involves a slip parameter that is hard to quantify and an unknown thickness of the constant-stress layer tacitly excluded from the water column. Blondeaux & Vittori (2005ab) avoided these drawbacks by adopting Dean's (1974) eddy viscosity profile combined with a no-slip condition at the bed. They assumed a time-independent eddy viscosity as their focus was on the inclusion of suspended load rather than the behaviour near $k = 0$ (which still showed positive growth rates). Recent numerical simulations of sand wave formation carried out with a k-epsilon model by Borsje et al. (2011) reveal both the depth- and time-dependency in the vertical eddy viscosity A_v. The profiles are nearly parabolic, whereas the M4 component of A_v is about half the residual component, with an almost identical parabolic vertical shape and a phase that is nearly constant over the water column. Borsje et al. (2011) found negative growth rates near $k = 0$, which was attributed to suspended load transport. Because of the different approaches, it is hard to interpret the conclusions from Komarova & Hulscher (2000), Blondeaux & Vittori (2005ab) and Borsje et al. (2011) in a unified manner.

1.4. Goal

The main goal of this study is to develop a new modelling framework that allows us to systematically investigate the implications of the (combined and separate) depth- and time-dependencies of the eddy viscosity on sand wave formation. Since numerical simulations are not suitable for such a task (time-consuming and difficult to analyse), we adopt an idealized modelling approach following a linear stability analysis. Since incorporating a k-epsilon model is unfeasible, we seek a parameterization of the key features of the eddy viscosity as found in the numerical simulations above (Borsje et al. 2011). This structure, parabolic in the vertical and with a significant M4-component, is further supported by the literature on estuarine hydrodynamics (McGregor 1972, Ianniello 1977). Our parameterization of the eddy viscosity allows for a spectral solution method, expressing the flow solution as a superposition of analytically obtained vertical profiles. This provides a computationally attractive alternative to the finite difference schemes used in other studies mentioned above. The innovation of our study is therefore twofold: (*i*) the inclusion of time-dependency in a depth-dependent vertical eddy viscosity representation in an idealized sandwave model, (*ii*) the use of a spectral solution method regarding the vertical structure of the flow.

2. MODEL FORMULATION

2.1. Hydrodynamic conservation laws

Consider tidal flow of angular frequency ω and typical depth-averaged flow velocity amplitude U in an offshore region of a shallow shelf sea, far away from coastal boundaries. The mean water depth H is of the order of tens of meters. Let $\mathbf{u} = (u,w)$ denote the flow velocity vector with components u and w in the (horizontal) x-direction and in the (vertical) z-direction, respectively. Ignoring rotation, we assume uniformity and zero flow in the y-direction. The free surface elevation is located at $z = \zeta$ around the still water level $z = 0$. The seabed is located at $z = -H + \eta$, where $\eta(x)$ represents the topographic undulations. These undulations are characterized by a bed amplitude h

that is small with respect to the water depth and a topographic length scale $L = 2\pi/k$ of about 10^2-10^3 m, i.e. well below the tidal wavelength.
Next, we assume hydrostatic pressure ($H \ll L$) and adopt the eddy viscosity concept as turbulence closure. Conservation of momentum and mass is then expressed by the 2DV (two-dimensional vertical) shallow water equations:

$$u_t + u\,u_x + w\,u_z = -g\,\zeta_x + A_h u_{xx} + [A_v N(\check{z})\,b(\omega t)\,u_z]_z, \qquad (1)$$

$$u_x + w_z = 0. \qquad (2)$$

Here, subscripted coordinates denote derivatives, g is the gravitational acceleration. The horizontal kinematic eddy viscosity, with typical magnitude A_h (in $m^2\ s^{-1}$), is assumed constant in time and space. Alternatively, the vertical kinematic eddy viscosity is written as the product of a dimensional reference value A_v (in $m^2\ s^{-1}$) and two dimensionless order one functions $N(\check{z})$ and $b(\omega t)$, which separately account for the vertical and temporal variations. This representation allows us to impose the eddy viscosity as obtained with the recent numerical model results of sandwave formation (Borsje et al. 2011).

2.2. Vertical eddy viscosity representation

Following McGregor (1972) and Ianniello (1977), we propose a parabolic profile of the vertical eddy viscosity (Figure 1), given by

$$N(\check{z}) = 1 - [\beta(\check{z}+\delta)]^2, \qquad (3)$$

with $\beta = (1 - R)^{1/2}/(1 - \delta)$. Equation (3) is a function of a re-scaled vertical coordinate $\check{z} = z/(H - \eta)$, ranging from -1 at the bed to 0 at the free surface. As shown in figure 1, N attains a small value R ($0 < R < 1$) at the bed (at $\check{z} = -1$) and reaches a maximum of unity near mid-depth (at $\check{z} = -\delta$ with $0 < \delta < 1$). Positive N-values everywhere in the water column are warranted by requiring $N(0) = 1 - \beta^2\delta^2 > 0$, which is equivalent to the constraint $\delta^{-1} > 1+(1-R)^{1/2}$. Default values used throughout this study are $R = 0.01$ and $\delta = 0.5$. Importantly, the dependency of $\check{z}$ on $\eta(x)$ implies that, in the case of a non-horizontal bed, the viscosity also depends on the horizontal coordinate x.

The temporal structure of the eddy viscosity is represented as a truncated Fourier series according to

$$b(\omega t) = \Sigma_p\, B_p \exp(\mathrm{i}p\omega t), \qquad (4)$$

with the summation ranging from $p = -P$ to P (with truncation number P) and complex coefficients B_p, contained in a column vector $\mathbf{B} = (B_{-P},\ldots,B_P)^T$ and satisfying $B_{-p} = B_p^*$ because $b(\omega t)$ is real (an asterisk denoting complex conjugation).

2.3. Boundary conditions and forcing

Regarding boundary conditions, we require zero perpendicular flow and no stress at the free surface as well as no slip at the bed. This implies $u_z = w = 0$ at $z = 0$ and $u = w = 0$ at $z = -H + \eta$, where we have adopted a rigid-lid approach, by which the upper boundary of the computational domain is set at $z = 0$ (rather than $z = \zeta$).
Recalling that k is the topographic wave number, we consider a spatial domain of length $L = 2\pi/k$ with spatially periodic boundary conditions. Finally, the problem is forced by a prescribed time-periodic pressure gradient. More precisely, the spatial average of the pressure gradient $g\zeta_x$ in equation (1) is prescribed. We adopt parameter values that are typical for sand wave regions in the North Sea. The dimensional vertical eddy viscosity magnitude is calculated from $A_v = c_d HU$ (Bowden et al. 1959), with drag coefficient $c_d = 2.5\times10^{-3}$.

2.4. Sediment transport and bed evolution

Finally, the bed evolves as a result of the divergence of the bed load sediment flux, which is modelled as a simple power law of the bed shear stress, supplemented with a bed slope correction. Defining the volumetric bed shear stress according to

$$\tau_b = A_v\, R\, b(\omega t)\, u_z \qquad \text{at } z = -H + \eta, \qquad (5)$$

we thus write

$$(1-\varepsilon_{por})\,\eta_t + [\,\alpha|\tau_b|^{\gamma}\,(\tau_b/|\tau_b| - \mu\,\eta_x)\,]_x = 0. \qquad (6)$$

Here, ε_{por} is the bed porosity (dimensionless). The term in square brackets is the bed load sediment flux, which contains three constants: a proportionality coefficient α (dimension $m^{2-2\gamma}\,s^{2\gamma-1}$), a dimensionless transport power $\gamma \sim 3/2$ and a

dimensionless (yet non-scaled) bed slope correction coefficient μ.

2.5. Scaling and linear stability analysis

Without reporting the details, we proceed by performing a scaling procedure. We thus reformulate our model in terms of dimensionless unknowns, and identify a set of dimensionless key parameters. Furthermore, it provides a justification of the so-called *quasi-stationary approach*, which allows us to consider the seabed fixed while solving the hydrodynamic problem. The seabed thus effectively evolves as a result of the tidally averaged divergence of the sediment flux. We therefore distinguish a 'fast' hydrodynamic time coordinate t (within tidal cycle) and a 'slow' morphodynamic time coordinate τ for the bed evolution (in the order of years).

Following the principles of a linear stability analysis, we then consider the bed profile as a small perturbation of a horizontal bed, i.e.

$$\eta = a(\tau) \cos kx\,, \qquad (7)$$

with a time-dependent bed amplitude $a(\tau)$ that is small with respect to the water depth. Defining $\varepsilon = a_{init}/H \ll 1$, we now expand the solution in powers of ε. This is symbolically represented as

$$\Psi = \Psi_0 + \varepsilon\, \Psi_1 + \text{h.o.t.}, \qquad (8)$$

where the vector Ψ contains (the dimensionless counterparts of) the flow velocity components, the free surface (gradient) and the sediment flux (higher order terms denoted by h.o.t.). Importantly, we must also expand the vertical structure of the eddy viscosity in powers of ε according to $N = N_0 + \varepsilon N_1 + \text{h.o.t.}$.

We subsequently solve for the basic state Ψ_0 and the perturbed state Ψ_1. In doing so, analogous to equation (4), we expand the temporal structure of the unknowns as a truncated Fourier series in time, where – for the flow components u and w – the associated complex coefficients are functions of the vertical coordinate z. The next step is to resolve the vertical structure of these quantities.

2.6. Superposition of vertical profiles

Essential and novel in our solution method is the fact that we express the horizontal flow velocity components as a superposition of vertical profiles for which the vertical stress term (the one in square brackets in equation (1)) simplifies considerably. These are:

- A finite number of *eigenfunctions* $\phi_m(\check{z})$, with corresponding eigenvalue λ_m, which satisfy $[N_0 \phi_{m,z}]_z + \lambda_m \phi_m = 0$, as well as $\phi_{m,z}(0) = \phi_m(-1) = 0$. These eigenfunctions, which form a complete set, can be expressed in terms of Legendre functions (e.g., Abramowitz & Stegun 1964; see Figure 2a).
- A so-called *residual flow's shape function* $\phi_{res}(\check{z})$, which satisfies $[N_0 \phi_{res,z}]_z = 1$ and $\phi_{res,z}(0) = \phi_{res}(-1) = 0$.
- A *constant function* $\phi_{bed}(\check{z}) = 1$, which (trivially) satisfies $[N_0 \phi_{bed,z}]_z = 0$ and $\phi_{bed,z}(0) = \phi_{bed}(-1) = 0$.

The inclusion of f_{res} and f_{bed} helps to improve the convergence properties of our method. With the aid of equation (2), the vertical flow velocity components are expressed as a superposition of the vertical integrals of the above profiles, denoted by Φ_m, Φ_{res} and Φ_{bed} (see Figure 2b). This implies that our flow solution exactly satisfies continuity in the entire water column. For sake of brevity, further details of the solution method to find Ψ_0 and Ψ_1 are omitted.

3. RESULTS

Simulations with our model indicate spectral convergence of our solution regarding the basic state, i.e. the flow over the flat bed. They also show the generation of higher harmonics due to the time-dependency in the vertical eddy viscosity. For example, if forced by an M2 pressure gradient, the time-varying eddy viscosity generates higher harmonics in the flow solution of the basic state. In classical stability models, this only occurs in the perturbed state as the result of the advective interaction (i.e., the terms $u_0\, u_{1,x}$ and $w_1\, u_{0,z}$ in the first order momentum equations) between the basic and the perturbed flow.

First results from the perturbed state, and hence the growth rates, which have not yet been investigated in detail for small R-values, display large flow gradients near the bed.

4. CONCLUSIONS

We have presented a new modelling framework that allows us to systematically investigate the implications of the (combined and separate) depth- and time-dependencies of the eddy viscosity on sand wave formation. Key features are the spectral method, that allows us to express the flow solution as a superposition of eigenfunctions and other vertical profiles.
First simulations with our model indicate favourable convergence properties (regarding basic state). The results from the perturbed state, and hence the growth rates, have not yet been investigated in detail.
Our simulations further show that in the near-bed region (where the eddy viscosity becomes small), the vertical flow gradients of the perturbed flow become very large. This is as expected, yet should be kept in mind when interpreting results from finite-difference numerical models with usually only a limited number of vertical grid points ('sigma-layers'). Finally, future extensions of our model may include the incorporation of suspended load, which is likely to require a different set of eigenfunctions.

5. REFERENCES

Abramowitz, M. & Stegun, I. A. 1964 Handbook of Mathematical Functions with Formulas, Graphs, and Mathematical Tables, 9th edn. New York: Dover.

Besio, G., Blondeaux, P., Brocchini, M. & Vittori, G. 2004 On the modeling of sand wave migration. J. Geophys. Res. 109, C04018.

Besio, G., Blondeaux, P. & Frisina, P. 2003 A note on tidally generated sand waves. J. Fluid Mech. 485, 171–190.

Blondeaux, P. & Vittori, G. 2005a Flow and sediment transport induced by tide propagation: 1. The flat bottom case. J. Geophys. Res. 110, C07020.

Blondeaux, P. & Vittori, G. 2005b Flow and sediment transport induced by tide propagation: 2. The wavy bottom case. J. Geophys. Res. 110, C08003.

Borsje, B. W., Roos, P. C., Kranenburg, W. M. & Hulscher, S. J. M. H. 2011 Modeling sand- wave formation in a numerical shallow water model. In RCEM 2011, 7th IAHR symposium on River, Coastal and Estuarine Morphodynamics, Beijing, China. (eds X Shao, Z Wang & G Wang). IAHR.

Bowden, K. F., Fairbairn, L. A. & Hughes, P. 1959 The distribution of shearing stresses in a tidal current. Geophys. J. R. Astr. Soc. 2, 288–305.

Dean, R. D. 1974 Aero report. Tech. Rep. 74-11. Imperial College, London.

Dodd, N., Blondeaux, P., Calvete, D., de Swart, H. E., Falqués, A., Hulscher, S. J. M. H., Rozynski, G. & Vittori, G. 2003 Understanding coastal morphodynamics using stability methods. J. Coast. Res. 19 (4), 839–865.

Gerkema, T. 2000 A linear stability analysis of tidally generated sand waves. J. Fluid Mech. 417, 303–322.

Hulscher, S. J. M. H. 1996 Tidal induced large-scale regular bed form patterns in a three-dimensional shallow water model. J. Geophys. Res. 101 (C9), 20,727–20,744.

Ianniello, J. P. 1977 Tidally induced residual currents in estuaries of constant breadth and depth. J. Mar. Res. 35, 755–786.

Komarova, N. L. & Hulscher, S. J. M. H. 2000 Linear instability mechanism for sand wave formation. J. Fluid Mech. 413, 219–246.

McGregor, R. C. 1972 The influence of eddy viscosity on the vertical distribution of velocity in the tidal estuary. Geophys. J. R. Astr. Soc. 29, 103–108.

Németh, A. A., Hulscher, S. J. M. H. & van Damme, R. M. J. 2007 Modelling offshore sandwave evolution. Cont. Shelf Res. 27 (5), 713–728.

Németh, A. A., Hulscher, S. J. M. H. & de Vriend, H. J. 2002 Modelling sand wave migration in shallow shelf seas. Cont. Shelf Res. 22 (18–19), 2795–2806.

Sterlini, F. M., Hulscher, S. J. M. H. & Hanes, D. M. 2009 Simulating and understanding sand wave variation: A case study of the Golden Gate sand waves. J. Geophys. Res. 114, F02007.

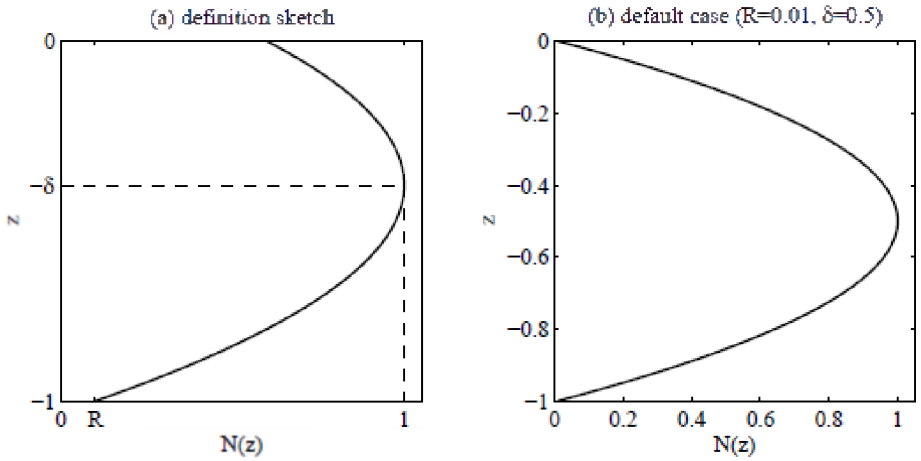

Figure 1. Parabolic viscosity profile $N(\check{z})$ according to equation (3): (a) general definition sketch showing the bottom value R and a maximum of unity at $\check{z} = -\delta$, (b) default case with $R = 0.01$ and $\delta = 0.5$.

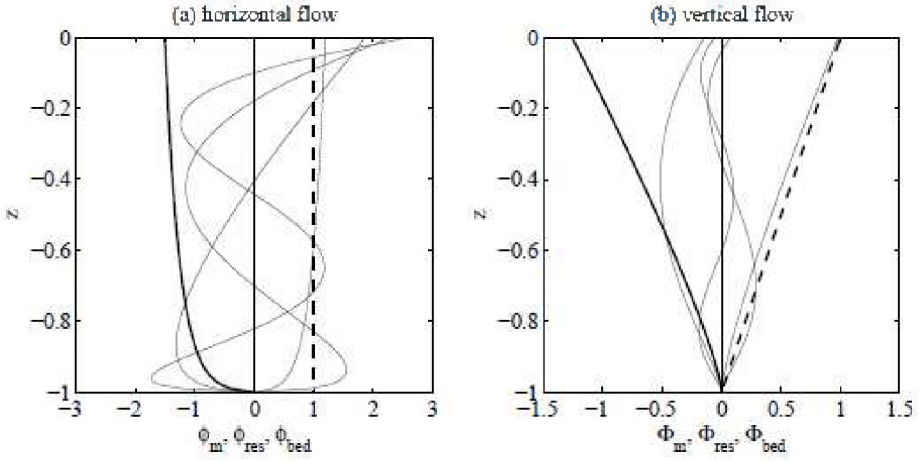

Figure 2. Overview of the functions used in the horizontal and vertical flow solution, respectively: (a) eigenfunctions ϕ_m (thin lines, $m = 1,2,3,4$), residual flow's shape function ϕ_{res} (thick line) and constant function ϕ_{bed}; (b) integrated eigenfunctions Φ_m (thin lines, $m = 1,2,3,4$) and integrated shape functions , Φ_{res} (thick solid line) and Φ_{bed} (thick dashed line). Parameter values $R = 0.01$, $\delta = 0.5$.